Plant Physiology and Biochemistry 148 (2020) 312–323

Contents lists available at ScienceDirect

Plant Physiology and Biochemistry

journal homepage: www.elsevier.com/locate/plaphy

Research article

Cadmium and arsenic-induced-stress differentially modulates Arabidopsis root architecture, peroxisome distribution, enzymatic activities and their nitric oxide content

D. Piacentini[a], F.J. Corpas[b], S. D'Angeli[a], M.M. Altamura[a,*], G. Falasca[a,*]

[a] Department of Environmental Biology, "Sapienza" University of Rome, Italy
[b] Group of Antioxidants, Free Radicals and Nitric Oxide in Biotechnology, Food and Agriculture, Department of Biochemistry, Cell and Molecular Biology of Plants, Estación Experimental del Zaidín, CSIC, C/Profesor Albareda 1, E-18008, Granada, Spain

ARTICLE INFO

Keywords:
Arsenic
Cadmium
CFP-PTS1 line
Nitric oxide
Oxidative stress
Peroxisomes
Root system

ABSTRACT

In plant cells, cadmium (Cd) and arsenic (As) exert toxicity mainly by inducing oxidative stress through an imbalance between the production of reactive oxygen species (ROS) and reactive nitrogen species (RNS), and their detoxification. Nitric oxide (NO) is a RNS acting as signalling molecule coordinating plant development and stress responses, but also as oxidative stress inducer, depending on its cellular concentration. Peroxisomes are versatile organelles involved in plant metabolism and signalling, with a role in cellular redox balance thanks to their antioxidant enzymes, and their RNS (mainly NO) and ROS. This study analysed Cd or As effects on peroxisomes, and NO production and distribution in the root system, including primary root (PR) and lateral roots (LRs). *Arabidopsis thaliana* wild-type and transgenic plants enabling peroxisomes to be visualized *in vivo*, through the expression of the 35S-cyan fluorescent protein fused to the peroxisomal targeting signal1 (PTS1) were used. Peroxisomal enzymatic activities including the antioxidant catalase, the H_2O_2-generating glycolate oxidase, and the hydroxypyruvate reductase, and root system morphology were also evaluated under Cd/As exposure. Results showed that Cd and As differently modulate these activities, however, catalase activity was inhibited by both. Moreover, Arabidopsis root system was altered, with the pollutants differently affecting PR growth, but similarly enhancing LR formation. Only in the PR apex, and not in LR one, Cd more than As caused significant changes in peroxisome distribution, size, and in peroxisomal NO content. By contrast, neither pollutant caused significant changes in peroxisomes size and peroxisomal NO content in the LR apex.

1. Introduction

Cadmium (Cd) and arsenic (As) soil contamination has become a global grave concern, due to the high toxicity, the no-biodegradability, and the persistence of these pollutants in the environment. In addition to causing losses in crop production, the bioaccumulation and biomagnification of these contaminants in the food chains represent a potential risk to human health (Ali et al., 2019). Plants, as sessile organisms, are constantly exposed to these toxic elements, which can negatively affect their growth and reproduction, eventually leading to their death (Nagajyoti et al., 2010). Root system is the first part of the plant to be exposed to toxic elements in the soil. Thus, the capacity of forming a proper root system, composed of both embryonic, i.e., primary root (PR) and post-embryonic roots, i.e., lateral roots (LRs), is fundamental for allowing plants to better cope with adverse environments, increasing their chance of survival. Cadmium is readily absorbed by the roots, it enters root cells as Cd^{2+} via cation channels for divalent cations or through Zn-specific ZIP transporters (Zare et al., 2018 and references therein). The heavy metal can be either translocated to aerial organs through xylem loading, or accumulated in the root cells, anyhow it leads to reactive oxygen and nitrogen species (ROS and RNS, respectively) production, root and shoot growth inhibition, genotoxicity, rate of photosynthesis reduction and alteration in the hormonal balance (Benavides et al., 2005; Fattorini et al., 2017; Huybrechts et al., 2019).

Abbreviations: CAT, catalase; CFP, cyan fluorescent protein; CLSM, confocal laser scanning microscopy; Col, Columbia; GOX, glycolate oxidase; H_2O_2, hydrogen peroxide; HPR, hydroxypyruvate reductase; LR, lateral root; LRD, lateral root density; LRL, lateral root length; LRP, lateral root primordium; NO, nitric oxide; NR, nitrate reductase; $O_2^{\cdot -}$, superoxide anion; PI, propidium iodine; PR, primary root; PCD, programmed cell death; PRL, primary root length; RNS, reactive nitrogen species; ROS, reactive oxygen species; WT, wild-type

* Corresponding authors.
E-mail addresses: mariamaddalena.altamura@uniroma1.it (M.M. Altamura), giuseppina.falasca@uniroma1.it (G. Falasca).

https://doi.org/10.1016/j.plaphy.2020.01.026
Received 23 October 2019; Received in revised form 18 December 2019; Accepted 17 January 2020
Available online 18 January 2020

Arsenic is a naturally occurring metalloid, with the oxidation states As (III) (arsenite) and As(V) (arsenate) as the most common and toxic forms in terrestrial environment (Zhao et al., 2009). Arsenate is taken up by the roots via phosphate transporters and interferes with phosphate metabolism, such as phosphorylation and ATP synthesis, generating oxidative stress and growth inhibition (Garg and Singla, 2011; Ronzan et al., 2018).

Peroxisomes are highly dynamic organelles actively involved in a plethora of plant processes, including abiotic stress responses, biosynthesis of phytohormones, generation of signalling molecules and antioxidant enzymes, and ROS/RNS homeostasis among others (Corpas et al., 2017, ; Corpas et al., 2019a,b; Hu et al., 2012; Sandalio et al., 2015). Their metabolism, number, size and morphology can change depending on the cell type, tissue, organism, developmental stage or environmental cue, such as the abiotic stress (Mano et al., 2002; Rodríguez-Serrano et al., 2009). In fact, changes in peroxisome number have been observed in *A. thaliana* after salt (Fahy et al., 2017), light (Desai and Hu, 2008), heavy metal (Rodríguez-Serrano et al., 2016) and H_2O_2 (Shibata et al., 2013) stresses. However, contradictory results have been reported regarding the type of changes that occur after stress exposure, as an increase or decrease in their number (Su et al., 2019 and references therein). In addition, less is known about peroxisome distribution inside root cells, and the study of their modifications in response to the heavy metal/metalloid toxicity in terms of distribution and morphology is lacking.

One of the most important function of peroxisomes is to contribute in the cellular redox homeostasis by controlling the levels of ROS/RNS, especially $O_2^{\bullet -}$, H_2O_2, NO and peroxynitrite (Corpas et al., 2019b and references therein). On the base of their cellular levels, ROS/RNS may act either as key molecules in perceiving environmental changes and triggering cell responses or, on the contrary, as highly reactive oxidant/nitrating species leading to cellular damages (Corpas et al., 2009; Sandalio et al., 2015). Peroxisomes can strongly regulate ROS/RNS levels either by producing or scavenging them, mainly activating the enzymatic and non-enzymatic antioxidant systems. Among all, catalase (CAT), glycolate oxidase (GOX) and hydroxypyruvate reductase (HPR) are typical peroxisome enzymes involved in ROS metabolism and cellular redox balance (Corpas et al., 2017; Yang et al., 2019). Catalase is the most important antioxidant enzyme, and the most abundant peroxisomal antioxidant enzyme (Su et al., 2018), involved in the degradation of the highly ROS H_2O_2 into H_2O and oxygen, and an increase of its activity, as part of the activation of the antioxidant defence system, helps plants to cope with several environmental stresses, like heavy metals (Palma et al., 1987; Zong et al., 2017), salinity (Mittova et al., 2004) and drought stress (Luna et al., 2004; Horváth et al., 2007; Signorelli et al., 2013), although a decrease of its activity under some stress conditions has also been reported (Mittova et al., 2003; Al Mahmud et al., 2017). Hydroxypyruvate reductase (HPR) and H_2O_2-producing glycolate oxidase (GOX) are key enzymes in photorespiration, one of the main metabolic processes controlling cellular redox homeostasis (Dellero et al., 2016). An enhancement of photorespiration rate during plant responses to stress conditions results in the production and accumulation of ROS (especially H_2O_2) mainly in peroxisomes, leading to oxidative stress and damage to cellular components (Voss et al., 2013).

One of the most important RNS is nitric oxide (NO), a gaseous free radical involved in several plant physiological processes both under normal and stress conditions (Kolbert et al., 2019 and references therein). Nitric oxide is produced in various cellular compartments such as mitochondria, chloroplasts and peroxisomes, as well as in the cytosol through the activity of nitrate reductase (NR) (Planchet and Kaiser, 2006). The presence of NO in peroxisomes has been corroborated by complementary techniques such as electron paramagnetic resonance spectroscopy using the spin trap $Fe(MGD)_2$ and fluorometric analysis with different fluorescence probes such as DAF-2 DA (Corpas et al., 2004). This peroxisomal NO seems to be generated by an L-arginine-dependent NO synthase (NOS)-like activity using NADPH as electron donor (Corpas et al., 2004; Corpas and Barroso, 2014).

Cellular NO generation has been found to provoke both beneficial and harmful effects, which depend predominantly on its local concentration, site of synthesis, spatial generation pattern, interaction with other molecules, and balance between its concentration and ROS along with antioxidant systems (Correa-Aragunde et al., 2015). Supporting this, it has been reported that the NO accumulation in *A. thaliana* PR, due to Cd exposure, contributes to the heavy metal-mediated inhibition of the root growth (Yuan and Huang, 2016), while, on the other hand, several studies pointed out the role of NO as a key signal molecule during root system formation and development, both in control and stress conditions (Schlicht et al., 2013; Correa-Aragunde et al., 2016). Although several studies demonstrated the role of peroxisomal NO in a plethora of physiological functions, as well as in the mechanism of response to abiotic stress conditions (Corpas et al., 2017 and references therein), less is known about peroxisome distribution inside root cells and tissues, and their modifications in response to the heavy metal/metalloid toxicity in terms of distribution, morphology and NO production (Nabi et al., 2019). Moreover, it is unknown whether, in the same root system, roots of different origin and with a different growth pattern, i.e. indeterminate for the embryonic PRs, and determinate for the post-embryonic LRs, react differently to Cd- and As-induced stresses in terms of peroxisome/NO behaviour.

Consequently, in this work, we evaluated the effects of 60 μM $CdCl_2$ or KH_2AsO_4, on the *A. thaliana* root system, particularly focusing on the response of peroxisomes in terms of their distribution and morphology in root cells, NO homeostasis and activity of some enzymes involved in ROS metabolism and in cellular redox balance. The ultimate goal was to assess whether the damage caused by Cd or As to the root architecture involved damage to peroxisomes and their metabolism. To this aim, *A. thaliana* wild type and transgenic plants expressing cyan fluorescent protein (CFP) fused to the *type 1 peroxisomal-targeting sig*nal (*PTS1*; *CFP-PTS1*) (Nelson et al., 2007), which enables peroxisomes to be visualized *in vivo*, were analysed with confocal laser scanning microscopy (CLSM) technique after heavy metal/metalloid treatments. The activities of CAT, GOX and HPR enzymes in response to treatments were also evaluated.

2. Materials and methods

2.1. Plant materials and growth conditions

One hundred fifty seeds of *A. thaliana* (L.) Heynh ecotype Columbia (Col, wild type, WT) and of transgenic plants expressing cyan fluorescent protein (CFP) fused to the *peroxisomal targeting signal 1* (*PTS1*) under the control of the *35S* promoter (*CFP-PTS1*) (Nelson et al., 2007) were surface sterilized for 5 min in a solution of 70% ethanol containing 0.1% SDS, then placed for 20 min in sterile water containing 20% bleach and 0.1% SDS, and then washed four times in sterile water. Afterwards, the seeds were sown on a medium containing full-strength Murashige and Skoog (Murashige and Skoog, 1962) (Sigma-Aldrich), 1% sucrose and 0.8% agar, at pH 5.6–5.8, supplemented or not (Control) with 60 μM $CdCl_2$ (Cd) or 60 μM KH_2AsO_4, (As) and kept at 4 °C in the dark for 2 days for vernalization. Cadmium level was chosen on the basis of both our preliminary results and of the results obtained by Yuan and Huang (2016). The As concentration was selected on the base of our preliminary unpublished data and, in particular, the concentration of 60 μM KH_2AsO_4 was chosen because it causes damage to Arabidopsis plants but it does not completely inhibit the growth of the root system.

Then, the plates were vertically incubated at long-day conditions (16 h light/8 h dark and 22 °C day/18 °C night) for 12 days. The light intensity was 100 μE m^{-2} s^{-1}.

2.2. Plant crude extracts and enzyme activity assays

One hundred and fifty 12-d-old Col seedlings grown in the presence or not of 60 μM $CdCl_2$ (Cd) or to 60 μM KH_2AsO_4 (As) were collected, ground with liquid nitrogen in pre-chilled mortars and pestles. The powder was suspended in a 5.10^4 μM Tris-HCl (pH 7.8, ratio 1:4; w/v) buffer containing 100 μM EDTA, 0.2% (v/v), Triton X-100 and 10% (v/v) glycerol. The homogenates were filtered and centrifuged at 27,000 g for 20 min and the supernatants were collected and used for the enzymatic assays.

The activity of CAT (EC 1.11.1.6) was spectrophotometrically estimated according to the method of Aebi (1984), by following the disappearance of H_2O_2 at 240 nm for 2 min at 25 °C. The reaction mixture contained 50 mM phosphate buffer (pH 7.0), 10.6 mM H_2O_2 and plant extract.

Glycolate oxidase (EC 1.1.3.1) activity was also determined spectrophotometrically by means of the formation of a glyoxylate-phenylhydrazone complex at 324 nm for 3 min at 25 °C in a reaction mixture containing 50 mM phosphate buffer (pH 8.0), 3 mM EDTA, 10 mM phenylhydrazine hydrochloride, 5 mM glycolic acid and plant extract (Kerr and Groves, 1975). Lastly, NADH-dependent hydroxypyruvate reductase (HPR; EC 1.1.1.29) activity was measured according to Schwitzguebel and Siegenthaler (1984) by monitoring the NADH oxidation at 340 nm.

Protein content was determined at 595 nm using the Bio-Rad protein assay (Hercules, CA), using a bovine serum albumin solution to prepare the standard curve.

2.3. Morphological and histological analyses of A. thaliana root system

Primary root length (PRL), lateral root length (LRL) and lateral root density (LRD) were evaluated in fifteen *A. thaliana* (WT) and *CFP-PTS1* seedlings per treatment and expressed in cm and mean number cm^{-1} (± SE), respectively. The plates containing the seedlings were scanned at 1200 dpi with Epson Perfection 2450 using Vuescan 9.0.94 software and morphologically analysed with RootNav image analysis tool (University of Nottingham, Ver. 1.8.1, 64-bit) (Pound et al., 2013). Primary roots and LRs were also treated with chloral hydrate solution (Weigel and Glazebrook, 2002), mounted on microscope slides and observed with Nomarski optics applied to a Leica DMRB optical microscope equipped with a Leica DC 500 camera.

Further, PRs and LRs were fixed, dehydrated, embedded in Technovit 7100 (Heraeus Kulzer, Germany), transversally sectioned (8 μm thickness) using the Microm HM 350 SV microtome (Microm,Walldorf, Germany), and stained with 0.05% toluidine blue according to Della Rovere et al. (2013). Histological sections were observed with a Leica DMRB microscope and the images acquired with a DC500 camera (Leica, Wetzlar, Germany).

2.4. Detection of NO in the root system of CFP-PTS1 transgenic seedlings using CLSM

For NO detection, fifteen Arabidopsis roots, taken from 12-days old *CFP-PTS1* seedlings grown in the presence or not of Cd or As, were incubated with 10 μM of the fluorescent probe 4-Amino-5-methylamino-2′,7′-difluorescein diacetate (DAF-FM DA, Calbiochem) prepared in 10 mM Tris-HCl (pH 7.4), for 1 h in darkness at room temperature (Corpas et al., 2006; Corpas and Barroso, 2014). The roots were then washed and left in the same buffer overnight to remove the excess of the probe, and afterwards mounted on a microscope slide and observed with a confocal laser scanning microscope (CLSM, Nikon C-1) using standard filters and collection modalities for CFP (excitation 433 nm; emission 475 nm). Fifteen roots per treatment were analysed. Each root was processed by CLSM obtaining an image resulting from 6 sections moving along Z axis at specific micrometric distances ranging from 13.25 to 17.7 μm depending on the magnification used. The images obtained were processed and the NO relative fluorescence quantified using ImageJ 1.52n software (https://imagej.nih.gov/ij). Nitric oxide fluorescence was acquired in red colour to avoid overlap with peroxisome signal that was in green colour.

Root peroxisomal NO was detected by merging the signals of *CFP-PTS1* construct (green spots) and DAF-FM DA (red spots) in the same field and analysing the resulting co-localization of the two fluorescence punctates. The images were acquired with a high magnification of the CLSM.

Considering that there is not overlap between the excitation/emission wavelengths of CFP (excitation 433 nm; emission 475 nm) and DAF-FM DA (excitation 495 nm and emission 515 nm) this allowed us to detect peroxisomal NO without artefacts due to the use of fluorochromes (Corpas et al., 2014).

2.5. Detection of NO and propidium iodide signal in the root system of wild-type seedlings using structured illumination technique

Nitric oxide signal was also observed in wild type PR apex, taken from 12-days old Col seedlings grown in the presence or not of Cd or As, after incubation with 10 μM of the fluorescent probe 4-amino-5-methylamino-2′,7′-difluorescein diacetate (DAF-FM DA, Calbiochem) solved in 10 mM Tris-HCl (pH 7.4), for 1 h in darkness at room temperature (Corpas et al., 2006; Corpas and Barroso, 2014). The roots were washed and mounted on a microscope slide, observed and the images acquired with an Axio Imager M2 fluorescence microscope (Zeiss, Germany) motorized on the 3 axes using filters with excitation at BP455-495 nm and emission at BP505-555 nm. The NO signal was in green colour.

The same root apices, used for NO detection, were also incubated for 5 min at room temperature with 15 μM of propidium iodide (PI) solution (Sigma) to evaluate cell death (Jones et al., 2016) and observed with a PI filter set (excitation BP510-560; emission LP590). Dead cells are in red color. The co-localization of the two fluorescence signals was set up.

Image z-stack scanning was performed with an Axiocam 512 (Zeiss) monochromatic camera and Apotome 2 (Zeiss) as fringe projection module used to remove the out of focus signal, to increase the sharpness, the contrast and the image resolution in the axial direction (structured illumination). Single plane images were obtained as Z-stack maximum projection using Zen 2.5 (Zeiss) image analysis software.

2.6. Detection of CFP-PTS1 signal and analysis of peroxisomes number and size in the roots

Peroxisomes were observed in fifteen roots of *CFP-PTS1* seedlings treated or not with Cd or As by CLSM as reported. Peroxisome size and number in the root tips were measured through the analysis of high magnification CLSM images using the Analyze Particles and the Find Maxima algorithms implemented in ImageJ 1.52n software and expressed as average size (μm^2) and as mean number $(10\ \mu m^2)^{-1}$, respectively. In order to better visualize peroxisome distribution and size inside root cells, *CFP-PTS1* roots treated or not with the pollutants were also stained with PI at 10 μg/ml in water for 5 min at room temperature and then observed under CLSM, with excitation/emission wavelengths of 597/637 nm. A representative workflow and image processing analysis with ImageJ 1.52n to get peroxisome number and size in the roots were respectively reported in Supplementary material S1 and S2.

2.7. Statistical analysis

The data were subjected to one-way analysis of variance (ANOVA) followed by Tukey's post-test through GraphPad Prism 6.07 software. Data represented in the table and figures are means of three replicates for each treatment.

3. Results

3.1. Cadmium and arsenic alter peroxisomal enzyme activities

In order to investigate the effects of 60 μM $CdCl_2$ (Cd) or 60 μM KH_2AsO_4 (As) on peroxisomal metabolism, the activity of three peroxisomal enzymes, the antioxidant catalase (CAT) and the two photorespiratory enzymes, H_2O_2-generating glycolate oxidase (GOX) and NADH-dependent hydroxypyruvate reductase (HPR) were analysed (Fig. 1).

Results showed that these enzyme activities in Arabidopsis seedlings grown in the presence of either Cd or As exhibited different modulations. In particular, CAT activity was significantly, and similarly, inhibited by both pollutants (between 35 and 42%) (Fig. 1 A). Contrary, both Cd and As triggered a significant increase of HPR activity, by 20% and 14% respectively in comparison to the Control seedlings (Fig. 1 B). Lastly, As treatment did not change GOX activity in comparison with the Control, while Cd significantly increased it (Fig. 1C).

These results pointed out that Cd and As differentially modulated the metabolism of peroxisomes by altering the activity of the analysed peroxisomal enzymes.

Considering that the roots are the target of Cd and As toxicity we decided to deepen the study of the effects of these pollutants on peroxisome distribution and metabolism in the root system.

3.2. Morphological effects of Cd or As on A. thaliana root system

The effects of Cd or As in the root system of *A. thaliana*, Col (wild type, WT) and transgenic (*CFP-PTS1*) seedlings were investigated, through a morphological analysis, on primary (PR) and lateral (LR) roots after 12 days of exposure to the pollutants, and the results were compared with those in the roots of the untreated seedlings (Control) (Fig. 2). The morphological data were obtained by the employment of the semi-automated software RootNav V1.8.1, because it represents a powerful tool to get detailed data about root architecture.

The effects of Cd and As on root morphology of *CFP-PTS1* seedlings were similar to those observed in the WT, thus only the data of the WT line are shown.

Exposure to Cd or As differently affected Arabidopsis PR growth, while caused similar effects on the lateral root length (LRL) and the lateral root density (LRD). Indeed, Cd inhibited ($P < 0.001$) Arabidopsis PR length by approx. 39% compared to the Control, whereas As significantly ($P < 0.001$) increased it (Fig. 2A–D). By contrast, both Cd and As induced a significant increase in LRD (Fig. 2D–E). However, many LRs remained at the lateral root primordium (LRP) stage under Cd treatment (Fig. 2 C, Inset). Altogether, morphological data indicate that both Cd and As induce alterations in the root system of *A. thaliana,* with different effects on the PR, and quite similar effects on the LRs.

3.3. Peroxisomes and NO distribution in A. thaliana primary and lateral roots is similar

The distribution of peroxisomes in the cells of LRs and PRs was evaluated as green spherical spots in *CFP-PTS1* seedlings by CLSM (Fig. 3 A, C, E, G). Results showed that both PRs and LRs exhibit a similar distribution of the peroxisome signal in the different regions of the organ (Fig. 3 A, C, E, G). Indeed, a weak *CFP-PTS1* signal was present in all the tissues of the differentiated regions of both root types (Fig. 3 A, E, Insets). However, moving from the differentiated zones towards the elongation and meristematic zones of PRs and LRs, the *CFP-PTS1* signal increased in all cells (Fig. 3 A, C, E, G), reaching the strongest intensity in the root meristem and cap cells (Fig. 3 C, G).

To detect NO localization in both root types, *CFP-PTS1* PRs and LRs were incubated with the fluorescence probe DAF-FM DA, which previously has been demonstrated to be a useful tool to detect and visualize the endogenous NO by CLSM in the different organs of different plant species (Corpas et al., 2006; Valderrama et al., 2007) (Fig. 3 B, D, F, H). As for the peroxisome signal, CLSM analysis showed that the pattern of NO distribution was similar in both PRs and LRs (Fig. 3 B, D and F, H, in comparison). In the differentiated zones of PRs and LRs the NO signal was weak in the vascular system and cortical parenchyma, but high in the rhizodermis (Fig. 3 B, F, Insets). In the elongation region of PR and LRs, NO signal decreased in all tissues, but mainly in the differentiating cortical parenchyma cells (Fig. 3 B, F). Finally, a weak signal was observed in the root apical meristem of both organ types (Fig. 3 B, F, arrowheads). An analysis at higher magnification showed that it was mainly localized in the root cap cells (Fig. 3 D and H).

To verify whether the peroxisomes were sources of NO in both LRs and PRs, the images showing NO as red spots (Fig. 4 A-C, arrowheads) and those showing peroxisomes as green spots (Fig. 4 D-F, arrowheads) were merged (Fig. 4G–I). When the green and the red spots co-localized, giving a yellow signal, we assumed that the NO production had a peroxisomal origin (Fig. 4 G-I, arrows and Insets).

The analysis was carried out in the apex of the PRs (Fig. 4 A, D), in the LR primordia (LRPs) formed in the mature zone of the PR (Fig. 4 B, E), and in the apex of the LRs (Fig. 4 C, F). The merge of images showed a very high overlapping of the two fluorescence punctates in the PR and in the LR apices and a high in the LRP (Fig. 4 G-I, Insets, arrows). On the contrary, a low overlapping of the two fluorescence punctates was observed in the PR mature zone near the LRP emergence, such as in the differentiated region of the LR (Fig. 4H–I).

These results demonstrated that both PRs and LRs have an analogous peroxisome and NO distribution, whose changes depend on the different region of the root. In this sense, PR and LR apex seems to be the most active zone for overlapping spots. In addition, the merging analysis demonstrated that peroxisomes are a source of NO in *A. thaliana* PR and LRs, and especially in their apices, including those of the LRPs.

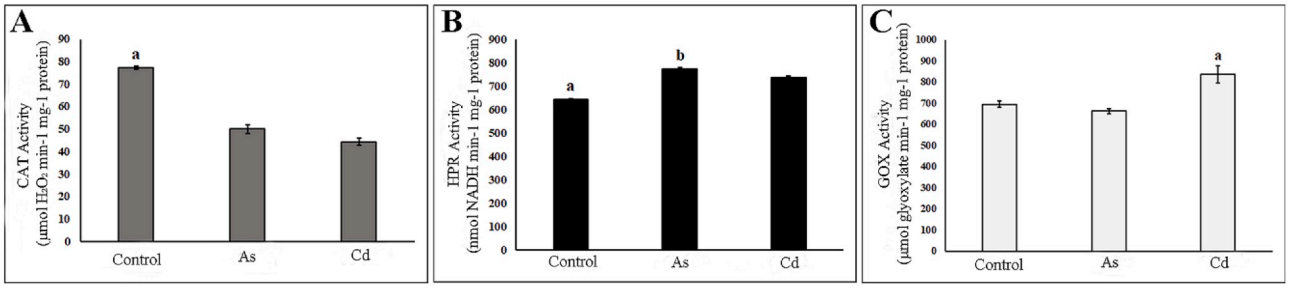

Fig. 1. Peroxisomal enzyme activities in 12-d-old *Arabidopsis thaliana* (Col) seedlings grown in MS medium not supplemented and supplemented with either 60 μM $CdCl_2$ (Cd) or 60 μM KH_2AsO_4 (As). **A**, Catalase (CAT) activity, expressed as μmol H_2O_2 min^{-1} mg^{-1} protein. **B**, hydroxypyruvate reductase (HPR) activity, expressed as nmol NADH min^{-1} mg^{-1} protein. **C**, Glycolate oxidase (GOX) activity, expressed as μmol glyoxylate phenylhydrazone min^{-1} mg^{-1} protein. Letter a shows statistical difference at least at $P < 0.05$ with respect to the other treatments. Letter b shows statistical difference at $P < 0.01$ level with respect to Cd. Columns followed by no letter are not significantly different. Data are means (± SE) of three technical replicates.

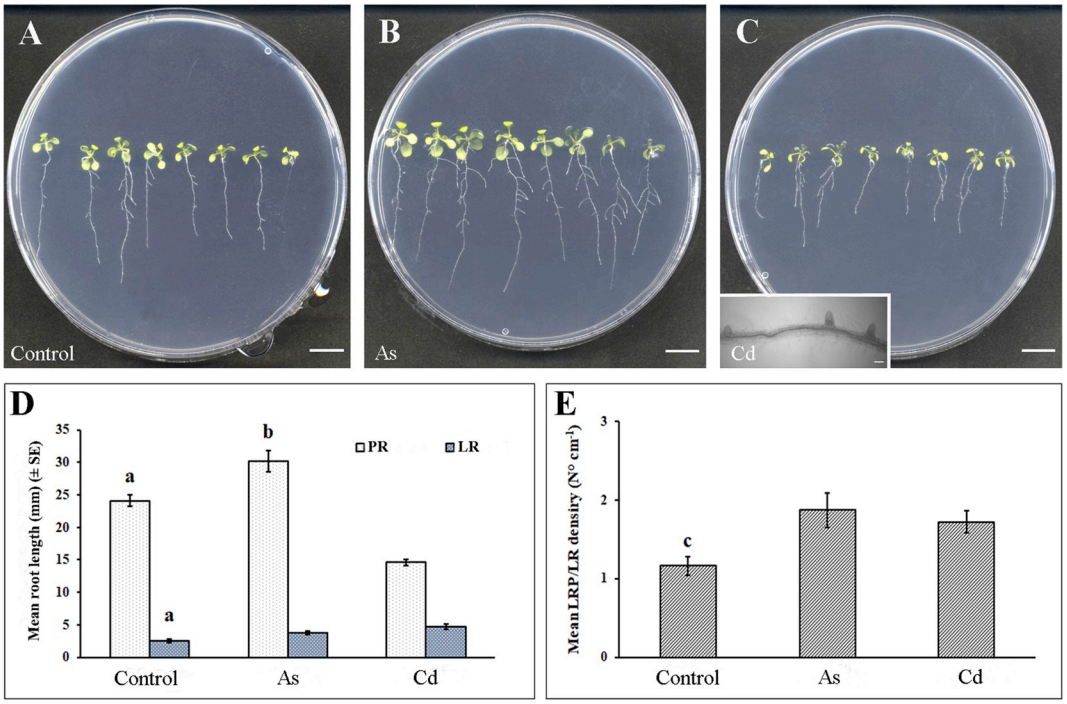

Fig. 2. Representative pictures of 12-d-old *Arabidopsis thaliana* (Col) seedlings grown in Murashige and Skoog medium not supplemented (panel **A**) and supplemented with either 60 μM KH_2AsO_4 (As) (panel **B**) or 60 μM $CdCl_2$ (Cd) (panel **C**, inset). Bars = 100 μm (inset in **C**), 1 cm (**A**-**C**). **D**-**E**, Means values (± SE) of primary and lateral roots length (**D**) and density of lateral root primordia (LRPs) and elongated lateral roots (LRs) (**E**) in Col seedlings exposed or not to As or Cd. Letters a and b show statistical differences ($P < 0.01$) within the same root type. Letter c shows statistical differences at least at $P < 0.05$ among the different treatments. Columns followed by no letter are not significantly different. N = 30.

3.4. Cadmium and As affect NO distribution in A. thaliana primary roots, but not in lateral roots

To verify whether Cd or As led to alterations in NO levels and distribution, the signal of the NO- fluorescent probe DAF-FM DA was investigated in both PR and LRs of *CFP-PTS1* seedlings after exposure to the heavy metal or the metalloid, and the NO fluorescence intensity quantified by using the ImageJ 1.52n software (Fig. 5).

The results showed that Cd significantly ($P < 0.001$, i.e. by approx. 45%) reduced the intensity of the NO fluorescence in the PR in comparison with that observed in the Control, but, surprisingly, not in the LRs (Fig. 5A–H). The As weakly, even if still significantly ($P < 0.05$), reduced NO signal in PR, but, as for Cd, did not cause significant changes in the LRs (Fig. 5A–H).

In addition, PRs and LRs exposed to Cd also showed an altered NO distribution pattern, with tissue differentiation occurring near the apex, and an intense and localized NO signal in the rhizodermis and hairs, in particular (Fig. 5 C, F).

Overall, these results indicate that Cd, more than As, reduce the NO level in PR of Arabidopsis seedlings, but not in the LR, even if in both root types Cd, and not As, alters NO distribution pattern.

3.5. Cadmium and As strongly reduce peroxisome distribution and peroxisomal NO production in the primary root but less in the lateral root

To investigate the consequences of Cd or As treatments on peroxisome distribution in the Arabidopsis root system, we studied the effects of these pollutants in both PR and LRs of the *CFP-PTS1* seedlings, and quantified the CFP-PTS1 fluorescence intensity and distribution using ImageJ 1.52n software (Fig. 6).

Arabidopsis PRs grown in the presence of Cd or As showed a significant ($P < 0.01$) reduction of the peroxisome signal intensity in comparison with the Control by 46% and 37%, respectively (Fig. 6 A-C, G). In addition, Cd significantly inhibited the *CFP-PTS1* significantly ($P < 0.01$), and reduced peroxisome signal in the LRs (Fig. 6 D, E, H).

Based on these results, we decided to focus further studies on the effects of Cd and As on NO production and peroxisome distribution in the apical region of both PRs and LRs. Peroxisomal NO production *in vivo,* after Cd or As treatments, was also detected by the analysis of merged images showing peroxisome and NO signal in the same regions of Arabidopsis *CFP-PTS1* PR and LR apices, after incubation with the DAF-FM DA probe (Fig. 7 A-C and G-I, arrows). The presence of an overlap between the two fluorescence punctates resulted into orange-yellow spots (Fig. 7 D-F and J-F, arrows). Results indicated that both Cd and As treatments altered peroxisomal NO accumulation in the tip of the PR of Arabidopsis seedlings, as shown by the reduction of the co-localized fluorescence punctates compared to the Control (Fig. 7 D-F, arrows). Notably, no difference in the number of co-localized fluorescence punctates was detected in the apices of the LRs exposed to both toxic elements with respect to those observed in the Control (Fig. 7 J-L, arrows).

Moreover, changes in peroxisome size and number in the apices of PRs and LRs of Arabidopsis seedlings grown in the presence of Cd or As were evaluated by measuring their size and by counting them using the commonly described “Analyze Particles” and “Find Maxima” automated tools of ImageJ 1.52n software (Fig. 8). A representative example of image processing which allows to quantify peroxisome size and number through these functions of the ImageJ 1.52n software is reported in Supplementary material S1 and S2.

Arabidopsis Cd-treated PRs showed a significant reduction of peroxisome number ($P < 0.05$) and at the same time a significant ($P < 0.01$) increase of their size compared to the Control, while no significant change was observed either in the number or in the dimensions of the peroxisomes in the LRs (Fig. 8 A, B, D, Insets in B, D). Arsenic did not change significantly peroxisome number and size both in the PRs and the LRs (Fig. 8 A, C, Inset in C).

Taken together, these results indicate that Cd and As alter peroxisome distribution and size, and peroxisomal NO production in *A.*

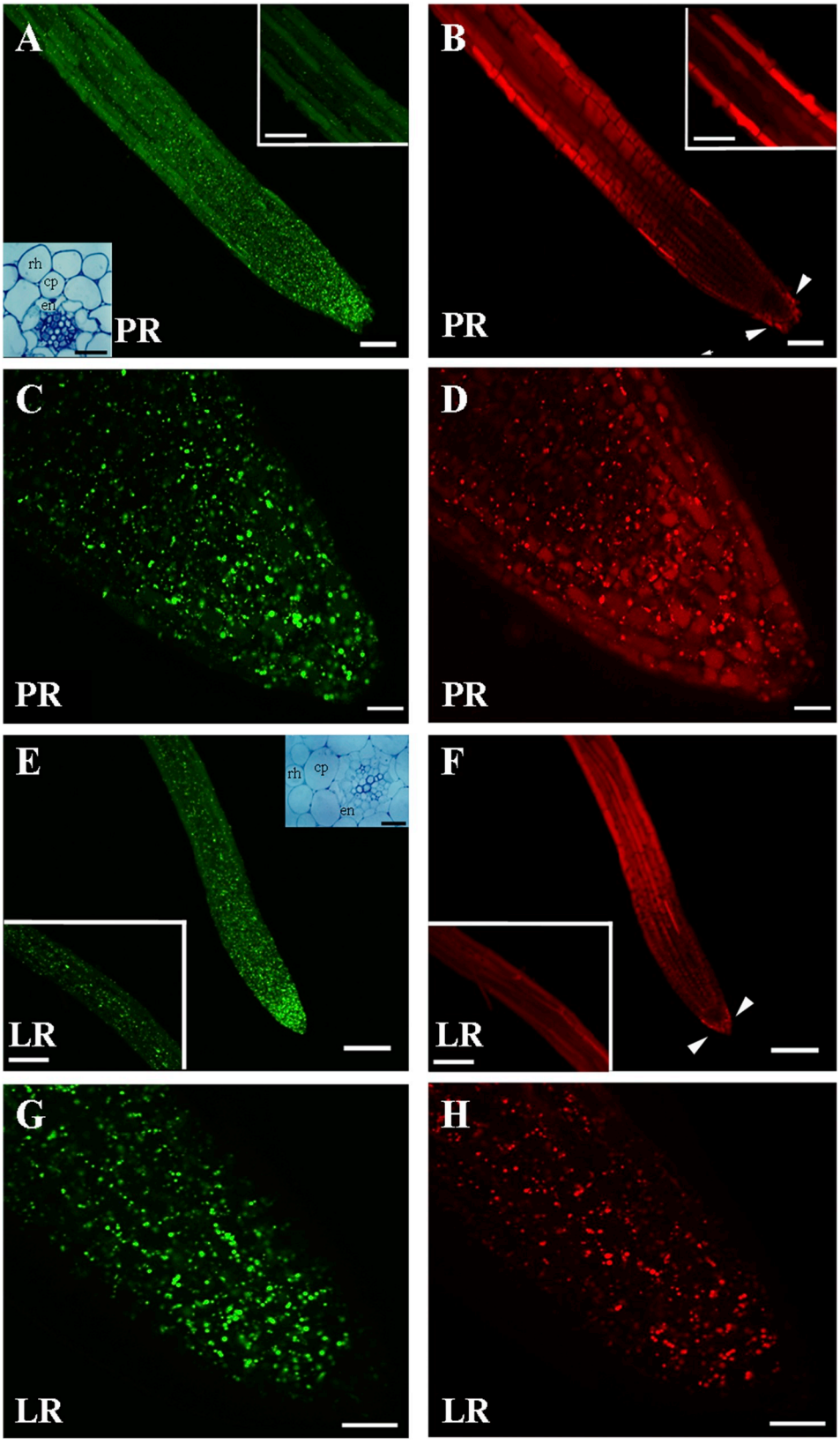

Fig. 3. Representative images illustrating the CLSM *in vivo* detection of peroxisomes (green colour) and NO (red colour) in primary and lateral roots of 12-d-old Arabidopsis seedlings expressing *CFP-PTS1* grown in Control conditions. Panels **A** to **D** correspond to primary root (PR). Panels **E** to **H** correspond to lateral root (LR). Each picture was the result of the superposition of 6 Arabidopsis root sections analysed by CLSM. Inset below in panel A and inset top in panel E show histological transections of PR and LR, respectively. rh, rhizodermis; cp, cortical parenchyma; en, endodermis. Bars = 5 μm (insets in **A**, **B**, **E**, **F**), 20 μm (**C**, **D**, **G**, **H**), 100 μm (**A**, **B**, **E**, **F**). (For interpretation of the references to colour in this figure legend, the reader is referred to the Web version of this article.)

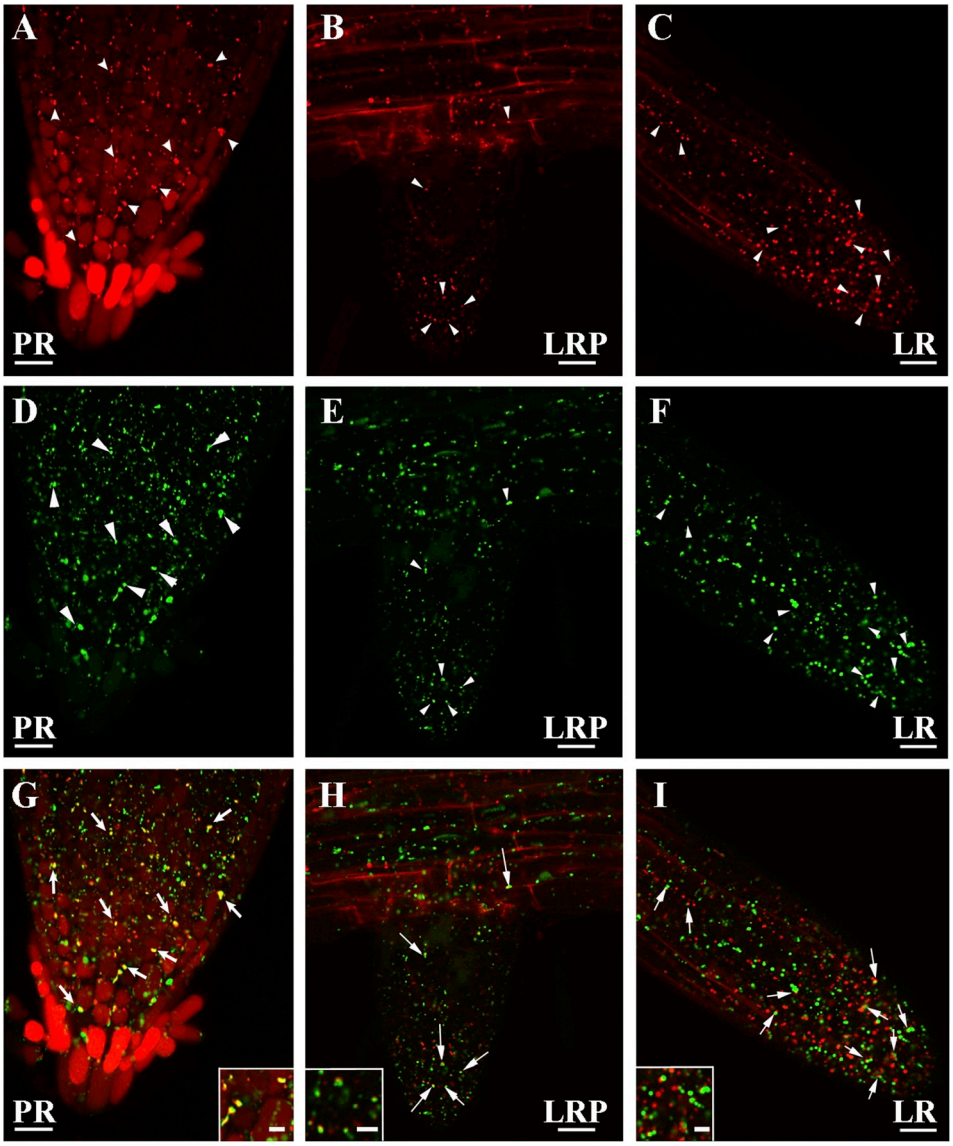

Fig. 4. Representative images illustrating the CLSM *in vivo* detection of NO (red colour) and peroxisomes (green colour) in primary (PR, **A**, **D**, arrowheads), lateral root primordium (LRP, **B**, **E**, arrowheads) and lateral roots (LR, **C**,**F**, arrowheads) of 12-d-old Arabidopsis seedlings expressing *CFP-PTS1* grown in Control conditions. **G-I**, merged images of the PR apex (**G**), PR mature zone with emerging LRP (**H**) and LR (**I**) showing co-localized fluorescence punctates (yellow, arrows) Each picture was the result of the superposition of 6 Arabidopsis root sections analysed by CLSM. Bars = 5 μm (inset in **G-I**), 20 μm (**A-I**). (For interpretation of the references to colour in this figure legend, the reader is referred to the Web version of this article.)

thaliana root system, with the PR as the specific target, and with Cd being more toxic than As for peroxisome distribution, size and NO content.

4. Discussion

4.1. Peroxisomes present in the apices of Arabidopsis PR and LRs are endogenous site source of NO

The data show that PRs and LRs have a comparable peroxisome and NO distribution, whose changes depend on the different region of the Arabidopsis root, and with the apex as the organ-zone richest in peroxisomes. In addition, peroxisomes are source of NO production, as shown by fluorescence merging analysis, independently of their presence in roots of embryonic (PR) or post-embryonic (LR) origin. It is known that most of peroxisomal matrix proteins have a C-terminal PTS1, and that must be imported in the organelle by the activity of a specific interacting receptor for this targeting signal (Reumann et al., 2007; Baker et al., 2016; Pan et al., 2019). By the use of transgenic plants expressing the cyan fluorescent protein (CFP) fused to the *PTS1* we can confirm that peroxisomes of Arabidopsis roots accumulate NO *in vivo*, and with the same pattern of distribution in the PR and LRs. Furthermore, a more in-depth analysis indicates that a low peroxisomal density occurs in the cells of the differentiated zones with respect to the meristematic cells of the root apex and to the cells of the root cap, in particular. As reported, the signal of peroxisomes, detected by analyzing *CFP-PTS1* line, is in the form of fluorescent spots. Thus, in the meristematic vs differentiated cells, regardless of their cell size, an increase in the number of fluorescent points represents with a high probability a greater number of fluorescent sources, i.e. peroxisomes. This means that the apical meristem needs peroxisomal functions under unstressed conditions, as also previously observed for the PR apex (Corpas et al., 2009). The observed high density of peroxisomes might be related to the known peroxisomal involvement in the production of phytohormones (e.g., auxins and jasmonates), which are necessary for the apical meristem functioning and maintenance (Corpas and Barroso, 2018, Schlicht et al., 2013, Della Rovere et al., 2013, 2015). Moreover, based on the peroxisome functioning in counteracting ROS production, the high density of peroxisomes in the apex might be interpreted as a mechanism of cytoprotection of the meristem cells against cellular ROS for maintaining their correct functionality, which is essential for a normal organ growth and tissue differentiation. In addition, it is known that the root cap cells undergo programmed cell death (PCD) before peeling off from the apex, and that the ROS produced in the peroxisomes play an important role in executing PCD (Fahy et al., 2017). Also in our experiments, events of PCD were detected in the cap cells, and in

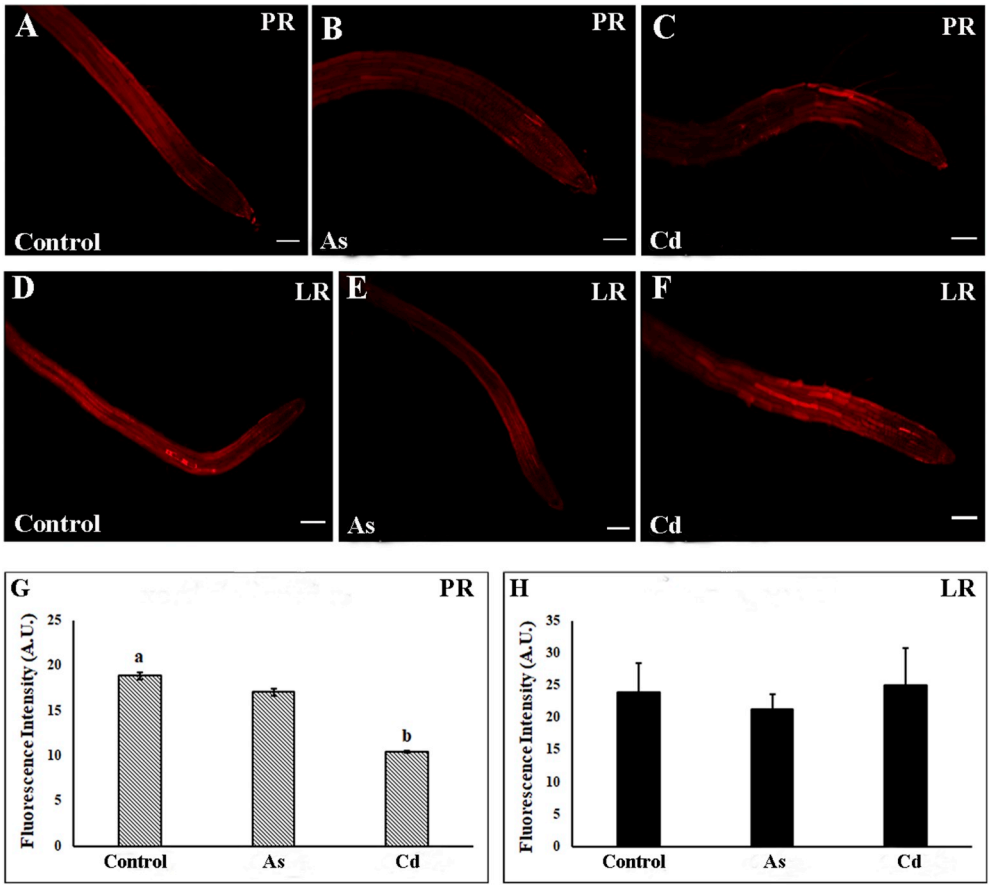

Fig. 5. Representative images illustrating the CLSM *in vivo* detection of NO (red colour) in primary (PR, **A-C**) and lateral roots (LR, **D-F**) of 12-d-old Arabidopsis seedlings expressing *CFP-PTS1* grown in the absence (Control) or presence or of 60 $CdCl_2$ (Cd) or 60 μM KH_2AsO_4 (As). Each picture was the result of the superposition of 6 Arabidopsis root sections analysed by CLSM. Bars = 100 μm. **G-H**, mean fluorescence intensity (± SE) of the CFP-PTS1 signal in PRs (**G**) and LRs (**H**). Letter a, statistically difference with respect to the other treatments for at least $P < 0.05$. Letter b, $P < 0.001$ difference with respect to As treatment. Columns followed by no letter are not significantly different. N = 15. (For interpretation of the references to colour in this figure legend, the reader is referred to the Web version of this article.)

the treated/untreated roots (Supplementary material S3). The differentiating cap cells also showed high peroxisome density and NO levels (Figs. 7–8, Supplementary material S3), possibly needed for sustaining in time ROS production and for signalling the PCD execution-time. Moreover, we observed that peroxisome density and NO levels decreased simultaneously with the start of PCD, and the As or Cd treatments anticipated these decreases, corroborating the role of peroxisome and its activity in PCD, but also highlighting that this organelle as a target of the pollutants (Supplementary material S3).

Moreover, we not only show high levels of NO in the cap cells which are preparing to death, but also an overlapping of NO and peroxisome signal in all the other apical cells of PR/LRs. This suggests that the NO produced by the meristem cells might be necessary for generating a nitrosative stress useful for PR/LR apical growth under normal conditions. In accordance, experimental evidence has been previously provided showing that NO production in Arabidopsis PR under normal conditions generates nitrosative stress by peroxynitrite (ONOO-) production (Corpas et al., 2009; Corpas and Barroso, 2014). Thus the present merging analysis demonstrates that peroxisomes are a source of NO in *A. thaliana* PR and in LRs and especially in their apices, thus contributing to the homeostatic control of NO in the root cells.

The CLSM analysis also showed that cellular NO was high in the rhizodermis of the mature root zone, where, however, there was quite no merging between peroxisomes and NO. Probably NO was high to sustain the polarized growth of the rhizodermal cells leading to hair formation, as also previously reported (Lombardo and Lamattina, 2018), but with no or a weak role of the NO produced by the peroxisomes in this process.

4.2. Cd and As can change the metabolism of peroxisomes and NO levels and distribution with the PR apex as the main target

Present morphological data indicate that both Cd and As induce alterations in the root system of *A. thaliana*, with different effects on the PR, and quite similar effects on the LRs. Cadmium and As alter peroxisomal ROS metabolism and NO production, with the PR apex as their main target, and with Cd more toxic than As. Negative effects of As (V) concentrations higher than that here used are known for the Arabidopsis roots (Leterrier et al., 2012; Fattorini et al., 2017), it is thus possible that the tested concentration (60 μM KH_2AsO_4) is not sufficient for causing important growth alterations, differently from Cd. It is also possible that the phosphate, present in the MS salt, interferes with the arsenate uptake, reducing the amount of As that accumulates in plant tissues, although it must be excluded that As uptake is completely inhibited as demonstrated in different plants, including Arabidopsis (Zanella et al., 2016; Ji et al., 2017). In fact, some effects were induced by this As level, i.e. a weak, but significant reduction in NO content and peroxisome fluorescence in the whole PR, and an important reduction in CAT activity in the whole seedling. These effects might indicate an As-induced stress in the PR causing a peroxisome reduction by pexophagy, a specialized form of autophagy (Lee et al., 2014; Young and Bartel, 2016), and, consequently, a reduction in peroxisome activities in the whole seedling. In accordance, events of pexophagy, mediated by CAT inhibition, are known in plant (Shibata et al., 2013) and animal systems (Lee et al., 2018). However, the PR apex did not show a reduction in peroxisome number, excluding pexophagy events in its cells, with this possibly resulting into a regular apex activity, and even an

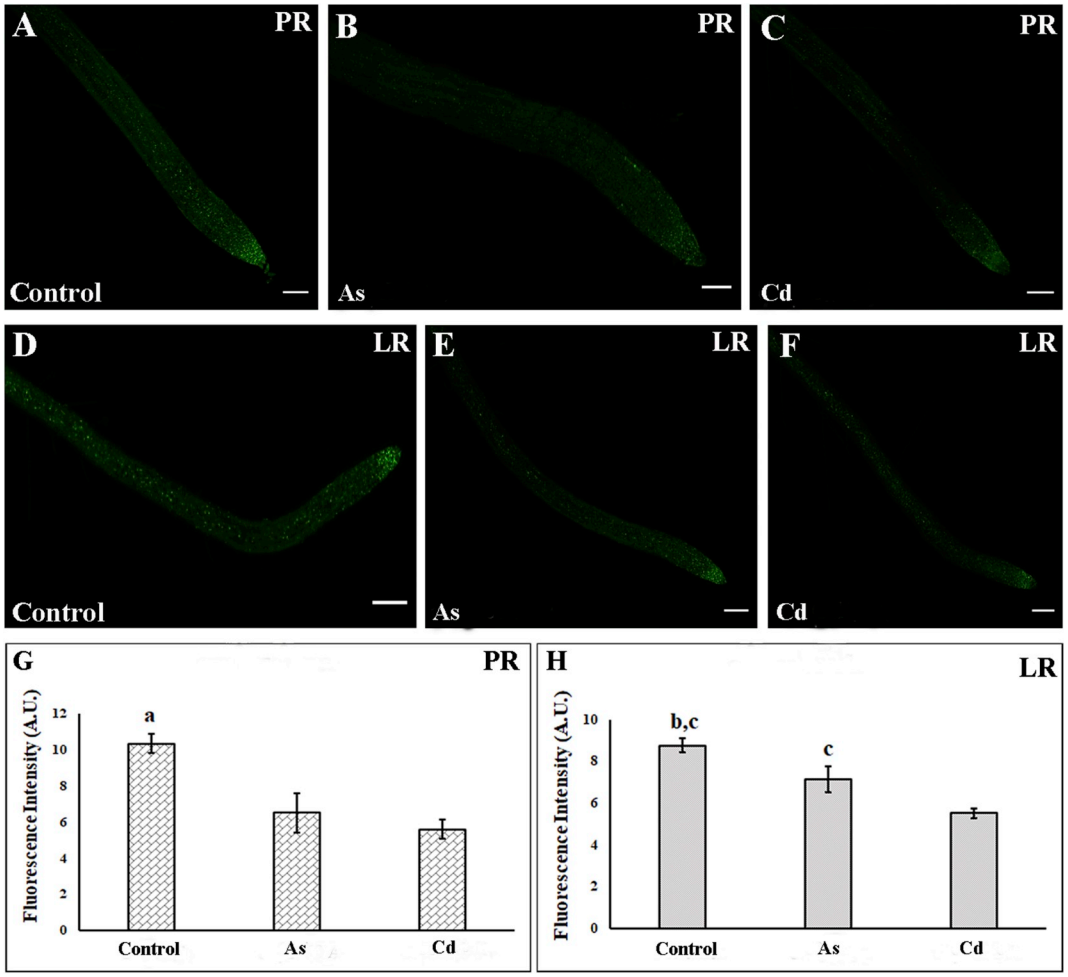

Fig. 6. Representative images illustrating the CLSM *in vivo* detection of peroxisome (green colour) in primary (PR, **A-C**) and lateral roots (LR, **D-F**) of 12-d-old Arabidopsis seedlings expressing *CFP-PTS1* grown in the absence (Control) or presence or of 60 μM $CdCl_2$ (Cd) or 60 μM KH_2AsO_4 (As). Each picture was the result of the superposition of 6 Arabidopsis root sections analysed by CLSM. Bars = 100 μm. **G-H**, mean fluorescence intensity (± SE) of the *CFP-PTS1* signal in PRs (**G**) and LRs (**H**). Letter a, $P < 0.01$ difference with respect to the other treatments. Letter b, $P < 0.01$ difference with respect to Cd. Letter c, $P < 0.01$with respect to Cd. Columns followed by no letter or by the same letter are not significantly different. N = 15. (For interpretation of the references to colour in this figure legend, the reader is referred to the Web version of this article.)

increase in the PR apex-governed elongation as a growth adaptive response, as in fact is observed.

By contrast, at the tested concentration (60 μM $CdCl_2$), Cd reduced PR length. This effect has been already documented in literature. In fact, it has been observed that PR elongation in Arabidopsis is inhibited after exposure to $CdCl_2$, with a progressive reduction in elongation from 50 to 150 μM $CdCl_2$ exposure (Yuan and Huang, 2016; Bruno et al., 2017), and that Cd toxicity depends on the impact on the quiescent centre (QC) of the embryonic in origin roots, such as in the PR apex of Arabidopsis or in embryonic adventitious root apices of rice (Bruno et al., 2017; Fattorini et al., 2017; Ronzan et al., 2018). Moreover, Cd-treated PRs are also known to exhibit a reduction of cap peripheral cells and delayed differentiation of the columella, with all these changes linked to an impairment of auxin accumulation at the apex, which in turn negatively affects the meristem activity (Yuan and Huang, 2016; Bruno et al., 2017). In accordance, we suppose that the observed Cd-caused reduction in PR elongation may be due to an altered QC, and related auxin accumulation, with this impairing the regular growth of the PR, as occurs for LRs and adventitious roots of the same plant (Fattorini et al., 2017). Moreover, a negative correlation among NO levels, auxin transport and root meristem activity has been also reported by Fernández-Marcos et al. (2011).

It has been also reported the NO participates in Cd-mediated inhibition of the PR apical meristem maintenance by reducing the activation of auxin signalling through a NO accumulation (Yuan and Huang, 2016). Moreover, under Cd (150 mM) stress, NO increases in Arabidopsis and is localized in peroxisomes and cytosol, participating in the generation of the nitro-oxidative stress caused by this heavy metal (Corpas and Barroso, 2014). In contrast, present results show that Cd reduced the NO content in the PR in comparison with the untreated Arabidopsis seedling but altered NO tissue-distribution pattern. Also peroxisome density was negatively affected by Cd, and the merging fluorescence analysis revealed that the Cd-induced reduction of cellular NO involved peroxisomes, and a reduction in peroxisome number and peroxisomal NO content. Consistently with these results, Cd changed the metabolism of peroxisomes by altering the activity of key peroxisomal enzymes (CAT, HPR and GOX) involved in cellular redox homeostasis and ROS metabolism. As reported, CAT is the most abundant peroxisomal antioxidant enzyme (Su et al., 2018) and a change in its activity highlights that the oxidative status of the peroxisome is affected. In our case, both Cd and As provoked a lower CAT activity, therefore a higher H_2O_2 content could be expected, sustaining the negative effects of the heavy metal and metalloid on peroxisome metabolism. Moreover both the other enzymes analysed, even if it are mainly involved in photorespiration, are differently modulated in the plant. In fact, whereas HPR activity increased with As, the GOX was

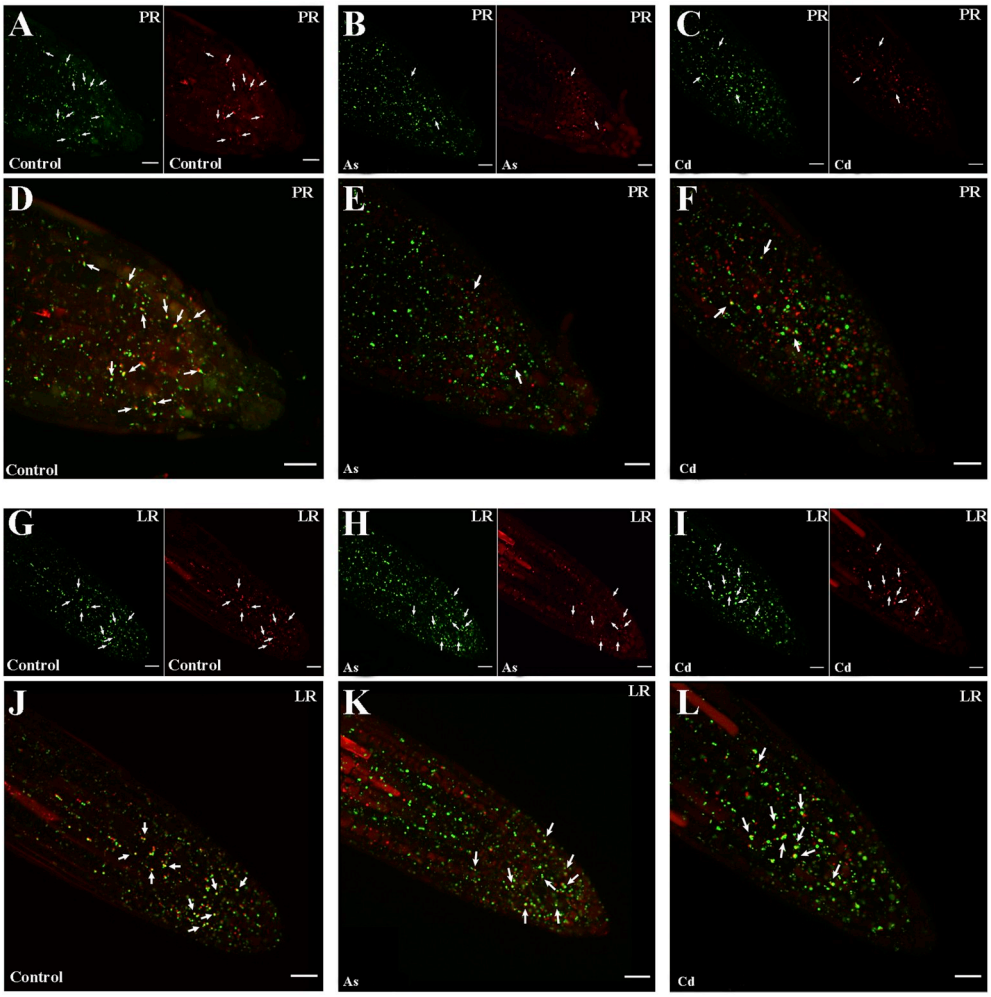

Fig. 7. Representative images illustrating the CLSM *in vivo* detection of peroxisome (green colour) and NO (red colour) in primary (PR, **A-C**) and lateral roots (LR, **G-I**) of 12-d-old Arabidopsis seedlings expressing *CFP-PTS1* grown in the absence (Control) or presence or of 60 μM $CdCl_2$ (Cd) or 60 μM KH_2AsO_4 (As). **D-F**, merged images of PR apices of Control, Cd and As showing co-localized fluorescence punctates (yellow-orange, arrows). **J-L**, merged images of LPR of Control, Cd and As showing co-localized fluorescence punctates (yellow-orange, arrows). Each picture was the result of the superposition of 6 Arabidopsis root sections analysed by CLSM. Bars = 20 μm. (For interpretation of the references to colour in this figure legend, the reader is referred to the Web version of this article.)

only affected with Cd, suggesting that the pollutants affected in different way their function in the peroxisomes. Considering that there is no antioxidant specific marker for peroxisomes in roots (Xu et al., 2015), that HPR and GOX have typical functions in the aerial organs, that the first and most intense damages caused by pollutants occur in the roots, our data show that the perception of the pollutants results into alterations in the peroxisomal antioxidant pool which start from the roots.

Taken together, results show that an adequate content of peroxisomal NO is necessary to the PR normal functioning, and that a reduction in peroxisomal NO production disturbs the apical meristem activity. This means that an adequate peroxisomal NO production might be necessary for normal development, but also for alleviating Cd toxicity in the PR apex. In accordance, under aluminium stress, NO alleviates aluminium repressed root elongation in the root apices of rye and wheat (He et al., 2012). We observed that LR formation was stimulated by Cd, even if many LRs remained at the LRP stage. In accordance, Cd increased LR and adventitious root density in Arabidopsis, and blocked growth at the primordium stage, when applied as $CdSO_4$ at the same 60 μM concentration (Fattorini et al., 2017). The enhancement of LR formation by Cd may be interpreted as a plant adaptive and acclimation strategy to the pollutant. Even if the few elongated LRs showed a Cd-induced reduction in peroxisome signal, as the PR, it is in fact notably that no appreciably change compared with the untreated Arabidopsis seedling occurred either in the peroxisome number or in the dimensions of the peroxisomes in the apices of the LRs/LRPs in response to the pollutant, and no reduction in NO content. However, the observation that many LRs remained at the primordium stage, i.e. were unable to elongate, may be due to a dysfunction of their QC caused by a disruption of auxin biosynthesis and transport by Cd, in accordance with previous observations with 60 μM $CdSO_4$ (Fattorini et al., 2017). Further research is necessary to clarify the relationship between peroxisomal NO production and QC activities in Arabidopsis LR apices in response to Cd and other soil pollutants.

5. Conclusions

At the tested concentration, Cd toxicity is higher that As toxicity. Moreover, Cd compromises the indeterminate growth pattern governed by PR apex, and from which PR regular elongation depends, by altering peroxisome distribution, size and biochemical activity, including peroxisomal NO production. The behaviour of the LRs and LRPs under both pollutants is different from that of the PR. In fact, Cd compromises the indeterminate growth pattern governed by PR apex, and from which PR regular elongation depends, by altering peroxisome distribution, size and biochemical activity, including peroxisomal NO production. However, the heavy metal increases LRP formation even if a lot of primordia fail to develop into elongated roots. This seems sufficient for

A Peroxisome number N° ($10\mu m^2$)$^{-1}$	PR	LR
Control	5.28 ± 0.30^a	5.11 ± 0.77
As	4.97 ± 0.21^a	4.98 ± 0.94
Cd	3.91 ± 0.21	4.73 ± 0.49
Peroxisome size (μm^2)	**PR**	**LR**
Control	2.38 ± 0.09^b	2.03 ± 0.14
As	2.06 ± 0.10^b	2.48 ± 0.35
Cd	2.96 ± 0.12	2.43 ± 0.17

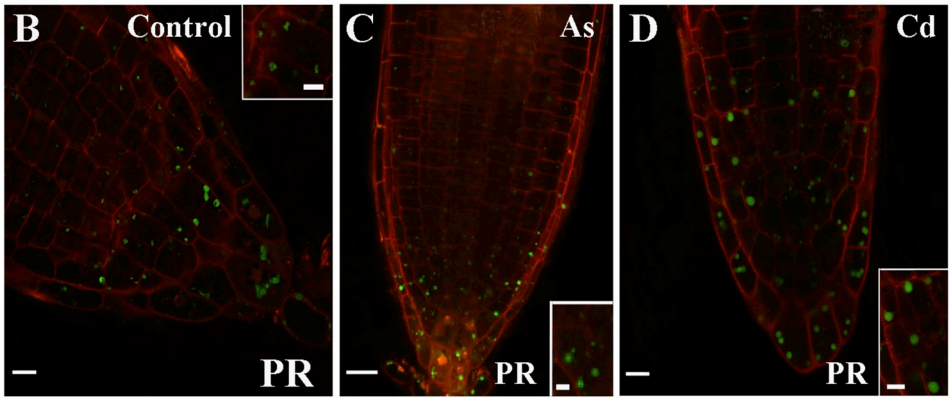

Fig. 8. A, Mean number and size of peroxisomes in the primary (PR) and lateral (LR) roots of *A. thaliana CFP-PTS1* seedlings grown in the absence (Control) or presence of 60 μM $CdCl_2$ (Cd) or 60 μM KH_2AsO_4 (As). Letter a, statistically difference with respect to Cd for at least $P < 0.05$; Letter b, statistically difference with respect to Cd for at least $P < 0.05$. Values with the same letter or no letter are not significantly different. N = 15. B-**D**, high magnification of CLSM images of PR apices treated with propidium iodide. Showing peroxisomes as green spots. Bars: 5 μm (insets **B**, **D**), 10 μm (**C**). (For interpretation of the references to colour in this figure legend, the reader is referred to the Web version of this article.)

LRs to compensate the peroxisomal-damaged embryonic PR, as a growth repair mechanism necessary to plant survival in the polluted context.

Declaration of competing interest

The authors declare no conflict of interest.

Acknowledgments

The authors gratefully thank Mr. Carmelo Ruiz-Torres for the help in the enzyme activity determination. We also thank Ms Alicia Rodríguez-Sánchez from the Microscopy Service (Estación Experimental del Zaidín, CSIC, Granada) for her valuable technical help during the confocal microscopy analyses. The research was founded by Sapienza University of Rome - Italy (Progetti per Avvio alla Ricerca to DP- AR11813F8C319B7) and by Ministry of Economy and Competitiveness, Spain (AGL201-104-P to FJC).

Appendix A. Supplementary data

Supplementary data to this article can be found online at https://doi.org/10.1016/j.plaphy.2020.01.026.

Authors' contribution

PD designed, carried out the research, analysed the data and performed the statistical analysis. CFJ and FG analysed and interpreted the data. DS carried out structured illumination microscope analyses. AMM discussed the results. AMM, FG and PD wrote the manuscript. All authors read and approved the manuscript.

References

Aebi, H., 1984. Catalase *in vitro*. Methods Enzymol. 105, 121–126. https://doi.org/10.1016/S0076-6879(84)05016-3.

Al Mahmud, J., et al., 2017. Maleic acid assisted improvement of metal chelation and antioxidant metabolism confers chromium tolerance in Brassica juncea L. Ecotoxicol. Environ. Saf. 144, 216–226. https://doi.org/10.1016/j.ecoenv.2017.06.010.

Ali, H., et al., 2019. Environmental chemistry and ecotoxicology of hazardous heavy metals: environmental persistence, toxicity and bioaccumulation. J. Chem. 2019https://doi.org/10.1155/2019/6730305. Article ID 6730305.

Baker, A., et al., 2016. Peroxisome protein import: a complex journey. Biochem. Soc. Trans. 44, 783–789. https://doi:.10.1042/BST20160036.

Benavides, M.P., et al., 2005. Cadmium toxicity in plants. Braz. J. Plant Physiol. 17, 21–34. https://doi.org/10.1590/S1677-04202005000100003.

Corpas, F.J., Barroso, J.B., 2014. Peroxynitrite ($ONOO^-$) is endogenously produced in Arabidopsis peroxisomes and is overproduced under cadmium stress. Ann. Bot. 113, 87–96. https://doi.org/10.1093/aob/mct260.

Corpas, F.J., Barroso, J.B., 2018. Peroxisomal plant metabolism–an update on nitric oxide, Ca^{2+} and the NADPH recycling network. J. Cell Sci. 131, jcs202978. https://doi.org/10.1242/jcs.202978.

Bruno, L., et al., 2017. In *Arabidopsis thaliana* cadmium impact on the growth of primary root by altering SCR expression and auxin-cytokinin cross-talk. Front. Plant Sci. 8, 1323. https://doi.org/10.3389/fpls.2017.01323.

Corpas, F.J., et al., 2004. Cellular and subcellular localization of endogenous nitric oxide in young and senescent pea plants. Plant Physiol. 136, 2722–2733 10.1104/pp.104.042812.

Corpas, F.J., et al., 2006. Constitutive arginine-dependent nitric oxide synthase activity in different organs of pea seedlings during plant development. Planta 224, 246–254. https://doi.org/10.1007/s00425-005-0205-9.

Corpas, F.J., et al., 2009. Peroxisomes are required for in vivo nitric oxide accumulation in the cytosol following salinity stress of Arabidopsis plants. Plant Physiol. 151, 2083–2094. https://doi.org/10.1104/pp.109.146100.

Corpas, F.J., et al., 2017. Plant peroxisomes: a nitro-oxidative cocktail. Redox Biol. 11, 535–542. https://doi.org/10.1016/j.redox.2016.12.033.

Corpas, F.J., et al., 2019a. Hydrogen sulfide (H_2S): a novel component in Arabidopsis peroxisomes which triggers catalase inhibition. J. Integr. Plant Biol. 61, 871–883. https://doi.org/10.1111/jipb.12779.

Corpas, F.J., et al., 2019b. Plant peroxisomes at the crossroad of NO and H_2O_2 metabolism. J. Integr. Plant Biol. 61, 803–816. https://doi.org/10.1111/jipb.12772.

Correa-Aragunde, N., et al., 2015. Nitric oxide is a ubiquitous signal for maintaining redox balance in plant cells: regulation of ascorbate peroxidase as a case study. J. Exp. Bot. 66, 2913–2921. https://doi.org/10.1093/jxb/erv073.

Correa-Aragunde, N., et al., 2016. The auxin-nitric oxide highway: a right direction in

determining the plant root system. In: Lamattina, L., García-Mata, C. (Eds.), Gasotransmitters in Plants. Springer International Publishing, Cham., Switzerland, pp. 117–136. https://doi.org/10.1007/978-3-319-40713-5_6.
Della Rovere, F., et al., 2013. Auxin and cytokinin control formation of the quiescent centre in the adventitious root apex of Arabidopsis. Ann. Bot. 112, 1395–1407. https://doi.org/10.1093/aob/mct215.
Della Rovere, F., et al., 2015. Arabidopsis SHR and SCR transcription factors and AUX1 auxin influx carrier control the switch between adventitious rooting and xylogenesis *in planta* and in *in vitro* cultured thin cell layers. Ann. Bot. 115, 617–628. https://doi.org/10.1093/aob/mcu258.
Dellero, Y., et al., 2016. Photorespiratory glycolate-glyoxylate metabolism. J. Exp. Bot. 67, 3041–3052. https://doi:.10.1093/jxb/erw090.
Desai, M., Hu, J., 2008. Light induces peroxisome proliferation in Arabidopsis seedlings through the photoreceptor phytochrome A, the transcription factor HY5 HOMOLOG, and the peroxisomal protein PEROXIN11b. Plant Physiol. 146, 1117–1127. https://doi.org/10.1104/pp.107.113555.
Fahy, D., et al., 2017. Impact of salt stress, cell death, and autophagy on peroxisomes: quantitative and morphological analyses using small fluorescent probe N-BODIPY. Sci. Rep. 7, 39069. https://doi.org/10.1038/srep39069.
Fattorini, L., et al., 2017. Cadmium and arsenic affect quiescent centre formation and maintenance in *Arabidopsis thaliana* post-embryonic roots disrupting auxin biosynthesis and transport. Environ. Exp. Bot. 144, 37–48. https://doi.org/10.1016/j.envexpbot.2017.10.005.
Fernández-Marcos, M., et al., 2011. Nitric oxide causes root apical meristem defects and growth inhibition while reducing PIN-FORMED 1 (PIN1)-dependent acropetal auxin transport. Proc. Natl. Acad. Sci. 108, 18506–18511. https://doi.org/10.1073/pnas.1108644108.
Garg, N., Singla, P., 2011. Arsenic toxicity in crop plants: physiological effects and tolerance mechanisms. Environ. Chem. Lett. 9, 303–321. https://doi.org/10.1007/s10311-011-0313-7.
He, H., et al., 2012. Nitric oxide signaling in aluminum stress in plants. Protoplasma 249, 483–492. https://doi.org/10.1007/s00709-011-0310-5.
Horváth, E., et al., 2007. Exogenous 4-hydroxybenzoic acid and salicylic acid modulate the effect of short-term drought and freezing stress on wheat plants. Biol. Plant. 51, 480–487. https://doi.org/10.1007/s10535-007-0101-1.
Hu, J., et al., 2012. Plant peroxisomes: biogenesis and function. Plant Cell 24, 2279–2303. https://doi.org/10.1105/tpc.112.096586.
Huybrechts, M., et al., 2019. Cadmium and plant development: an agony from seed to seed. Int. J. Mol. Sci. 20, 3971. https://doi:.10.3390/ijms20163971.
Ji, R., et al., 2017. Calcium-dependent protein kinase CPK31 interacts with arsenic transporter AtNIP1;1 and regulates arsenite uptake in *Arabidopsis thaliana*. PLoS One 12 (3), e0173681. https://doi.org/10.1371/journal.pone.0173681.
Jones, K., et al., 2016. Live-cell fluorescence imaging to investigate the dynamics of plant cell death during infection by the rice blast fungus *Magnaporthe oryzae*. BMC Plant Biol. 16, 69. https://doi.org/10.1186/s12870-016-0756-x.
Kerr, M.W., Groves, D., 1975. Purification and properties of glycolate oxidase from *Pisum sativum* leaves. Phytochemistry 14, 359–362. https://doi.org/10.1016/0031-9422(75)85090-4.
Kolbert, Z., et al., 2019. A forty year journey: the generation and roles of NO in plants. Nitric Oxide 93, 53–70. https://doi:.10.1016/j.niox.2019.09.006.
Lee, H.N., et al., 2014. Degradation of plant peroxisomes by autophagy. Front. Plant Sci. 5, 139. https://doi.org/10.3389/fpls.2014.00139.
Lee, J.N., et al., 2018. Catalase inhibition induces pexophagy through ROS accumulation. Biochem. Biophys. Res. Commun. 501, 696–702. https://doi.org/10.1016/j.bbrc.2018.05.050.
Leterrier, M., 2012. Arsenic triggers the nitric oxide (NO) and S-nitrosoglutathione (GSNO) metabolism in Arabidopsis. Environ. Pollut. 166, 136–143. https://doi.org/10.1016/j.envpol.2012.03.012.
Lombardo, M.C., Lamattina, L., 2018. Abscisic acid and nitric oxide modulate cytoskeleton organization, root hair growth and ectopic hair formation in Arabidopsis. Nitric Oxide 80, 89–97. https://doi.org/10.1016/j.niox.2018.09.002.
Luna, C.M., et al., 2004. Drought controls on H_2O_2 accumulation, catalase (CAT) activity and CAT gene expression in wheat. J. Exp. Bot. 56, 417–423. https://doi.org/10.1093/jxb/eri039.
Mano, S., et al., 2002. Distribution and characterization of peroxisomes in Arabidopsis by visualization with GFP: dynamic morphology and actin-dependent movement. Plant Cell Physiol. 43, 331–341. https://DOI:.10.1093/pcp/pcf037.
Mittova, V., et al., 2003. Up-regulation of the leaf mitochondrial and peroxisomal antioxidative systems in response to salt-induced oxidative stress in the wild salt-tolerant tomato species *Lycopersicon pennellii*. Plant Cell Environ. 26, 845–856. https://doi.org/10.1046/j.1365-3040.2003.01016.x.
Mittova, V., et al., 2004. Salinity up-regulates the antioxidative system in root mitochondria and peroxisomes of the wild salt-tolerant tomato species *Lycopersicon pennellii*. J. Exp. Bot. 55, 1105–1113. https://doi.org/10.1093/jxb/erh113.
Murashige, T., Skoog, F., 1962. A revised medium for rapid growth and bio assays with tobacco tissue cultures. Physiol. Plant. 15, 473–497. https://doi.org/10.1111/j.1399-3054.1962.tb08052.x.
Nabi, R.B.S., et al., 2019. Nitric oxide regulates plant responses to drought, salinity, and heavy metal stress. Environ. Exp. Bot. 161, 120–133. https://doi.org/10.1016/j.envexpbot.2019.02.003.
Nagajyoti, P.C., et al., 2010. Heavy metals, occurrence and toxicity for plants: a review. Environ. Chem. Lett. 8, 199–216. https://doi.org/10.1007/s10311-010-0297-8.
Nelson, B.K., et al., 2007. A multicolored set of in vivo organelle markers for co-localization studies in Arabidopsis and other plants. Plant J. 51, 1126–1136. https://doi.org/10.1111/j.1365-313X.2007.03212.x.
Palma, J.M., et al., 1987. Increased levels of peroxisomal active oxygen-related enzymes in copper-tolerant pea plants. Plant Physiol. 85, 570–574. https://doi.org/10.1104/pp.85.2.570.
Pan, R., et al., 2019. Peroxisomes: versatile organelles with diverse roles in plants. New Phytol. https://doi.org/10.1111/nph.16134.
Planchet, E., Kaiser, W.M., 2006. Nitric oxide production in plants: facts and fictions. Plant Signal. Behav. 1, 46–51. https://doi.org/10.4161/psb.1.2.2435.
Pound, M.P., et al., 2013. RootNav: navigating images of complex root architectures. Plant Physiol. 162, 1802–1814. https://doi.org/10.1104/pp.113.221531.
Reumann, S., et al., 2007. Proteome analysis of Arabidopsis leaf peroxisomes reveals novel targeting peptides, metabolic pathways, and defense mechanisms. Plant Cell 19, 3170–3193. https://doi.org/10.1105/tpc.107.050989.
Rodríguez-Serrano, M., et al., 2009. Peroxisome dynamics in Arabidopsis plants under oxidative stress induced by cadmium. Free Radic. Biol. Med. 47, 1632–1639. https://doi.org/10.1016/j.freeradbiomed.2009.09.012.
Rodríguez-Serrano, M., et al., 2016. Peroxisomes extend peroxules in a fast response to stress via a reactive oxygen species-mediated induction of the peroxin PEX11a. Plant Physiol. 171, 1665–1674. https://doi.org/10.1104/pp.16.00648.
Ronzan, M., et al., 2018. Cadmium and arsenic affect root development in *Oryza sativa* L. negatively interacting with auxin. Environ. Exp. Bot. 151, 64–75. https://doi.org/10.1016/j.envexpbot.2018.04.008.
Sandalio, L.M., Romero-Puertas, M.C., 2015. Peroxisomes sense and respond to environmental cues by regulating ROS and RNS signalling networks. Ann. Bot. 116, 475–485. https://doi.org/10.1093/aob/mcv074.
Schlicht, M., et al., 2013. Indole-3-butyric acid induces lateral root formation via peroxisome-derived indole-3-acetic acid and nitric oxide. New Phytol. 200, 473–482. https://doi.org/10.1111/nph.12377.
Schwitzguebel, J.P., Siegenthaler, P.A., 1984. Purification of peroxisomes and mitochondria from spinach leaf by Percoll gradient centrifugation. Plant Physiol. 75, 670–674. https://doi.org/10.1104/pp.75.3.670.
Shibata, M., et al., 2013. Highly oxidized peroxisomes are selectively degraded via autophagy in Arabidopsis. Plant Cell 25, 4967–4983. https://doi.org/10.1105/tpc.113.116947.
Signorelli, S., et al., 2013. Water stress induces a differential and spatially distributed nitro-oxidative stress response in roots and leaves of *Lotus japonicus*. Plant Sci. 201–202, 137–146. https://doi.org/10.1016/j.plantsci.2012.12.004.
Su, T., et al., 2018. The Arabidopsis catalase triple mutant reveals important roles of catalases and peroxisome derived signaling in plant development. J. Integr. Plant Biol. 60, 591–607. https://doi.org/10.1111/jipb.12649. Epub 2018 Jun 5.
Su, T., et al., 2019. Dynamics of peroxisome homeostasis and its role in stress response and signaling in plants. Front. Plant Sci. 10, 705. https://doi.org/10.3389/fpls.2019.00705.
Valderrama, R., et al., 2007. Nitrosative stress in plants. FEBS Lett. 581, 453–461. https://doi.org/10.1016/j.febslet.2007.01.006.
Voss, I., et al., 2013. Emerging concept for the role of photorespiration as an important part of abiotic stress response. Plant Biol. 15, 713–722. https://doi.org/10.1111/j.1438-8677.2012.00710.x.
Weigel, D., Glazebrook, J., 2002. Arabidopsis: a Laboratory Manual, first ed. CSHL Press, New York. https://doi.org/10.1017/S0016672302215852.
Xu, Y., et al., 2015. Root antioxidant mechanisms in relation to root thermotolerance in perennial grass species contrasting in heat tolerance. PLoS One 10, e0138268. https://doi.org/10.1371/journal.pone.0138268.
Yang, Z., et al., 2019. Analysis of catalase mutants underscores the essential role of CATALASE2 for plant growth and day length-dependent oxidative signalling. Plant Cell Environ. 42, 688–700. https://doi.org/10.1111/pce.13453.
Young, P.G., Bartel, B., 2016. Pexofagy and peroxisomal protein turnover in plants. Biochem. Biophys. Acta 1863, 999–1005. https://doi.org/10.1016/j.bbamcr.2015.09.005.
Yuan, H.M., Huang, X., 2016. Inhibition of root meristem growth by cadmium involves nitric oxide-mediated repression of auxin accumulation and signalling in Arabidopsis. Plant Cell Environ. 39, 120–135. https://doi.org/10.1111/pce.12597.
Zanella, L., et al., 2016. Overexpression of *AtPCS1* in tobacco increase arsenic and arsenic plus cadmium accumulation and detoxification. Planta 243, 605–622. https://doi.org/10.1007/s00425-015-2428-8.
Zare, A.A., et al., 2018. Root uptake and shoot accumulation of cadmium by lettuce at various Cd:Zn ratios in nutrient solution. Ecotoxicol. Environ. Saf. 148, 441–446. https://doi.org/10.1016/j.ecoenv.2017.10.045.
Zhao, F.J., et al., 2009. Arsenic uptake and metabolism in plants. New Phytol. 181, 777–794. https://doi.org/10.1111/j.1469-8137.2008.02716.x.
Zong, H., et al., 2017. Protective effect of chitosan on photosynthesis and antioxidative defense system in edible rape (*Brassica rapa* L.) in the presence of cadmium. Ecotoxicol. Environ. Saf. 138, 271–278. https://doi.org/10.1016/j.ecoenv.2017.01.009.